

Extra tuning sections for ESKF

October 26, 2021

10.8 Tuning IMU measurements

The process of tuning for the IMU comes down to assessing which noise processes are present in the sensors, as we assume the measurements to be a better description of reality than some dynamic model. In addition we need to consider how to accommodate the errors we introduce in the integration.

For another read on setting IMU parameters, the Autonomous Systems Lab at ETHZ has made a nice one on their Kalibr github page.wiki¹

10.8.1 Summary

There is in essence 3 processes that you need to take into account for a high grade IMU. This is the white measurement noise, the bias, and the bias instability. For the gyroscope the white noise and random walk (Wiener) bias could be termed angle random walk and rate random walk, respectively. For accelerometer this becomes velocity random walk and acceleration random walk.

For IMU, one often uses what is known as Allan deviation to assess which processes are present to which degree. The Allan deviation is related to the autocorrelation function, but behaves better for many signals due to using differences of the averaged signal at different times.

In particular, when looking at a log-log plot of the Allan deviation, different processes dominates in different regions. White measurement noise, bias instability, and random walk (Wiener process) shows up as a -0.5 slope, flat region, and 0.5 slope, respectively, towards the beginning, middle, and end of the plot, respectively. Bias instability precess is problematic to estimate, and is said to represent the minimal residual bias after estimation, in terms of standard deviations. Finding the parameters for these three processes boils down to

- Fitting a *negative* 0.5 slope line at the beginning of the plot, the size of the white noise can be read off this line at 1.
- The bias instability can be read off as the lowest point of the plot.
- Fitting a *positive* 0.5 slope line towards the end of (or even beyond) the plot, the size of the random walk noise can be read off this line at 3.

In addition, there might be quantization and ramp noise that behaves as a unit negative and positive Allan-deviation slope, respectively. See Figure 10.3 for an example.

Gauss-Markov looks like a random walk up until about 80% of the time constant, and like (scaled) white noise after about 400% of the time constant. If its driving noise has size σ , and the time constant is T , the random walk and white noise asymptotes meets at $\sqrt{3}T \approx 1.73T$ times the time constant, of a value of $\frac{\sigma\sqrt{T}}{\sqrt{3}} = 0.76\sigma\sqrt{T}$, whereas the true curve reaches its peak at $1.89T$ with a value of $0.437\sigma\sqrt{T}$. See Figure 10.2.

One could argue that no sensor exhibits true random walk in the long term, and that it should be more appropriately modeled as a Gauss-Markov with ‘very’ long time constant, or something else entirely. Which to choose might depend the application. Additionally, one or several Gauss-Markov processes could be added to model some of the bias instability by setting their peaks in the log-log Allan deviation plot at the regions where the combination of only white noise and random walk becomes to low compared to the plot of the real data. Note that a Gauss-Markov that explains the bias instability well enough will have problems with the larger long term bias variations and vice versa.

10.8.2 Allan Variance

The Allan variance for a process is, simply put, a method of representing rms random drift error as a function of averaging time. For a process $\Omega(t)$ it is defined as the time average of the difference of two averages of the process. We denote the time average of a function as

¹<https://github.com/ethz-asl/kalibr/wiki/IMU-Noise-Model>

$\langle f(t) \rangle = \lim_{T \rightarrow \infty} \frac{1}{2T} \int_{-T}^T f(t) dt$. We also denote the τ length average of the process Ω at time t as $\bar{\Omega}_\tau(t) = \frac{\int_{t-\tau}^{t+\tau} \Omega(t) dt}{\tau}$, and the difference operator $\Delta_\tau \Omega(t) = \Omega(t + \tau) - \Omega(t)$. With this the Allan variance is defined as

$$\sigma_\Omega^2(\tau) = \frac{1}{2} \langle (\Delta_\tau \bar{\Omega}_\tau(\tilde{t}))^2 \rangle = \frac{1}{2} \langle (\bar{\Omega}_\tau(\tilde{t} + \tau) - \bar{\Omega}_\tau(\tilde{t}))^2 \rangle \quad (10.1)$$

which can equivalently be written as either of the following

$$= \frac{1}{2} \left\langle \left(\frac{\int_{\tilde{t}}^{\tilde{t}+\tau} \Delta_\tau \Omega(t) dt}{\tau} \right)^2 \right\rangle = \frac{1}{2\tau^2} \left\langle \left(\int_{\tilde{t}+\tau}^{\tilde{t}+2\tau} \Omega(t) dt - \int_{\tilde{t}}^{\tilde{t}+\tau} \Omega(t) dt \right)^2 \right\rangle. \quad (10.2)$$

Expanding the square on the first line we get

$$\sigma_\Omega^2(\tau) = \frac{1}{2} (\langle \bar{\Omega}_\tau^2(\tilde{t} + \tau) \rangle + \langle \bar{\Omega}_\tau^2(\tilde{t}) \rangle - 2 \langle \bar{\Omega}_\tau(\tilde{t} + \tau) \bar{\Omega}_\tau(\tilde{t}) \rangle). \quad (10.3)$$

We now let $\hat{R}_{xx}(\tau) = \langle x(\tilde{t} + \tau)x(\tilde{t}) \rangle$ be the time average autocorrelation. We note that for most reasonable processes, and any of those we would like to study here, that $\langle \bar{\Omega}_\tau^2(\tilde{t} + \tau) \rangle = \langle \bar{\Omega}_\tau^2(\tilde{t}) \rangle$. With this we get

$$\sigma_\Omega^2(\tau) = \hat{R}_{\bar{\Omega}\bar{\Omega}}(0) - \hat{R}_{\bar{\Omega}\bar{\Omega}}(\tau) \quad (10.4)$$

However, through often occurring wide sense ergodicity² (mean-ergodic and autocovariance-ergodic) of $\bar{\Omega}_\tau(t)$, the time averaged autocorrelation is equal to the standard autocorrelation, i.e. $\hat{R}_{xx}(\tau) = \langle x(\tilde{t} + \tau)x(\tilde{t}) \rangle = \mathbb{E}[x(\tilde{t} + \tau)x(\tilde{t})] = R_{xx}(\tau)$. For such processes the above becomes

$$\sigma_\Omega^2(\tau) = R_{\bar{\Omega}_\tau \bar{\Omega}_\tau}(0) - R_{\bar{\Omega}_\tau \bar{\Omega}_\tau}(\tau). \quad (10.5)$$

From the definitions we have that

$$R_{\bar{\Omega}_\tau \bar{\Omega}_\tau}(\tilde{\tau}) = \mathbb{E} \left[\frac{\int_{\tilde{t}}^{\tilde{t}+\tau} \Omega(t) dt}{\tau} \frac{\int_{\tilde{t}+\tilde{\tau}}^{\tilde{t}+\tau+\tilde{\tau}} \Omega(s) ds}{\tau} \right] = \frac{1}{\tau^2} \int_{\tilde{t}}^{\tilde{t}+\tau} \int_{\tilde{t}+\tilde{\tau}}^{\tilde{t}+\tau+\tilde{\tau}} \mathbb{E}[\Omega(t)\Omega(s)] dt ds \quad (10.6)$$

$$= \frac{1}{\tau^2} \int_{\tilde{t}}^{\tilde{t}+\tau} \int_{\tilde{t}+\tilde{\tau}}^{\tilde{t}+\tau+\tilde{\tau}} R_{\Omega\Omega}(t-s) dt ds. \quad (10.7)$$

This can simplify the calculations, as we typically know the autocorrelation of the processes we want to find the Allan variance for.

Another potentially simplifying form comes from difference form on the second line. Again we assume wide sense ergodicity, but now of $\Delta_\tau \Omega(t)$. Now we get a second form for theoretical calculations as

$$\sigma_\Omega^2(\tau) = \frac{1}{2\tau^2} \int_{\tilde{t}}^{\tilde{t}+\tau} \int_{\tilde{t}}^{\tilde{t}+\tau} \mathbb{E}[\Delta_\tau \Omega(t) \Delta_\tau \Omega(s)] ds dt = \frac{1}{2\tau^2} \int_{\tilde{t}}^{\tilde{t}+\tau} \int_{\tilde{t}}^{\tilde{t}+\tau} R_{\Delta_\tau \Omega \Delta_\tau \Omega}(t, s) ds dt \quad (10.8)$$

Visualization

To visualize one often plots the Allan deviation, the square root of the Allan Variance, denoted $\sigma_\Omega(\tau)$ on a log-log plot. To see which curve this becomes in a x - y plane one can define $x = \log_{10} \tau$ and

$$y(x) = \log_{10}(\sigma_\Omega(\tau)) = \log_{10}(\sigma_\Omega(10^x)), \quad (10.9)$$

and simplify the result, which for several processes of interest becomes simple straight lines.

²The ergodicity claim actually need some further justification, but it happens to give the correct results here.

■ **Example 10.3 — White noise.** When $\Omega(t) = \sigma_a v(t)$ is a white noise process, we get the autocorrelation $R_{\Omega\Omega}(\tau) = \delta(\tau)$. Performing the integrals we get $R_{\Omega\Omega}(0) = \frac{\sigma_a^2}{\tau}$ and $R_{\Omega\Omega}(\tau) = 0$, so $\sigma_\Omega^2(\tau) = R_{\Omega\Omega}(0) = \frac{\sigma_a^2}{\tau}$.

Defining $x = \log_{10} \tau$ and

$$y(x) = \log_{10}(\sigma_v(\tau)) = \log_{10}\left(\frac{\sigma_a}{\sqrt{\tau}}\right) = \log_{10}(\sigma_a) - 0.5 \log_{10}(\tau) = \log_{10}(\sigma_a) - 0.5x, \quad (10.10)$$

we get a line with slope -0.5 . The value of (the logarithm in x - y coordinates of) σ_a can readily be read of a plot at $\tau = 1 \Leftrightarrow x = 0$. ■

■ **Example 10.4 — Wiener process.** When the process is a Wiener process, such that $\Omega(t) = \sigma_a W(t)$, the second form is simpler to work with. The τ time length increments of a Wiener process are i.i.d. and statistically equal to $W(\tau)$. Since we are looking at two different intervals, the autocorrelation of these increments is therefore $R_{\Delta\tau\Omega\Delta\tau\Omega}(s, t) = \max(0, \min(t + \tau, s + \tau) - \max(t, s)) = \max(0, \tau - |t - s|)$ and hence wide sense stationary. Performing the integration yields ($|t - s| \leq \tau$ so the ‘max’ disappears, the integrand is independent of the specific joint origin of t and s , and the absolute value is symmetric about 0)

$$\sigma_\Omega^2(\tau) = \frac{\sigma_a^2}{2\tau^2} \int_0^\tau \int_0^\tau \tau - |t - s| dt ds = \frac{\sigma_a^2}{2\tau^2} (\tau^3 - 2 \int_0^\tau \int_0^t t - s ds dt) = \frac{\sigma_a^2}{2\tau^2} (\tau^3 - \frac{\tau^3}{3}) = \frac{\sigma_a^2 \tau}{3} \quad (10.11)$$

On a log-log scale plot we get $y(x) = \log_{10}(\sigma_W(\tau)) = \log_{10}(\sigma_a) + 0.5(x - \log_{10}(3))$, a line with slope 0.5. The value for σ_a can again readily be read of this plot at $\tau = 3$. ■

■ **Example 10.5 — Gauss-Markov.** The Gauss-Markov process is given by $\dot{x} = -\frac{1}{T}x + \sigma_a v$, where v is unit white noise. Assuming that the process it has been running forever (or sufficiently long for the initial value to be numerically insignificant), its autocorrelation function is $R_{xx}(\tau) = \frac{\sigma_a^2 T}{2} e^{-\frac{|\tau|}{T}}$. Using the first method we can find

$$R_{\bar{x}_\tau \bar{x}_\tau}(\tau) = \frac{1}{\tau^2} \int_\tau^{2\tau} \int_0^\tau \frac{\sigma_a^2 T}{2} e^{-\frac{t-s}{T}} ds dt = \frac{\sigma_a^2 T^3}{2\tau^2} (e^{-\tau/T} - e^{-2\tau/T})(e^{\tau/T} - 1) \quad (10.12)$$

$$= \frac{\sigma_a^2 T^3}{2\tau^2} (1 - 2e^{-\tau/T} + e^{-2\tau/T}) \quad (10.13)$$

and

$$R_{\bar{x}_\tau \bar{x}_\tau}(0) = \frac{1}{\tau^2} \int_0^\tau \int_0^\tau \frac{\sigma_a^2 T}{2} e^{-\frac{|t-s|}{T}} ds dt = \frac{\sigma_a^2 T}{2\tau^2} \int_0^\tau 2 \int_0^t e^{-\frac{t-s}{T}} ds dt = \frac{\sigma_a^2 T^2}{\tau^2} \int_0^\tau 1 - e^{-\frac{t}{T}} dt \quad (10.14)$$

$$= \frac{\sigma_a^2 T^2}{\tau^2} (\tau - T(1 - e^{-\frac{\tau}{T}})). \quad (10.15)$$

This results in

$$\sigma_x^2(\tau) = R_{\bar{x}_\tau \bar{x}_\tau}(0) - R_{\bar{x}_\tau \bar{x}_\tau}(\tau) \quad (10.16)$$

$$= \frac{\sigma_a^2 T^2}{\tau} \left(1 - \frac{T}{2\tau} \left(3 - 4e^{-\frac{\tau}{T}} + e^{-\frac{2\tau}{T}} \right) \right). \quad (10.17)$$

For small and large values this function has neat approximations. For very large $\frac{\tau}{T}$, we have $\frac{T}{2\tau} \left(3 - 4e^{-\frac{\tau}{T}} + e^{-\frac{2\tau}{T}} \right) \ll 1$, so $\sigma_x^2(\tau) \approx \frac{\sigma_a^2 T^2}{\tau}$, which is a white noise signal. For very small $\frac{\tau}{T}$, a third order Taylor series of the exponentials shows that $\sigma_x^2(\tau) = \frac{\sigma_a^2 \tau}{3} + o((\frac{\tau}{T})^2)$, which is a Wiener

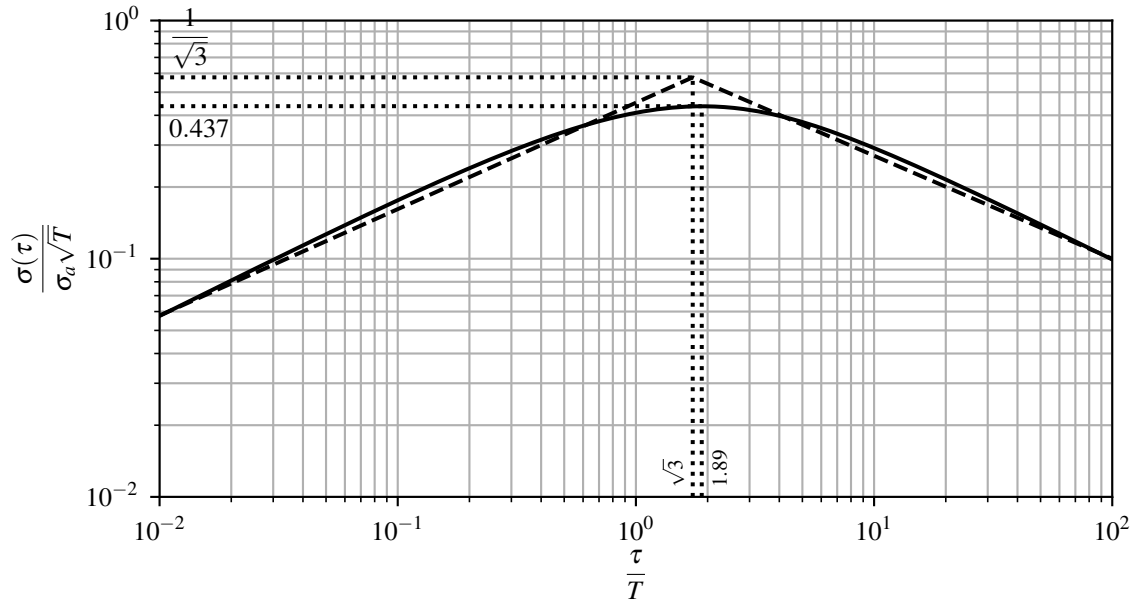


Figure 10.2: Allan deviation plot of a Gauss-Markov process with asymptotes.

signal. The Allan deviation has a peak for $\frac{\tau}{T} = 1.89$ at $0.437\sigma_a\sqrt{T}$. The approximation asymptotes in the log-log plot of the Allan deviation meets for $\frac{\tau}{T} = \sqrt{3} \approx 1.73$ at $\frac{\sigma_a\sqrt{T}}{\sqrt{3}} \approx 0.760\sigma_a\sqrt{T}$. ■

■ **Example 10.6 — Bias instability.** Bias instability is often defined as the lowest value of the Allan deviation plot. It is modeled as a constant Allan variance/deviation value for averaging values greater than some ‘small enough’ value, and acting as a ramp ($\propto \tau$) for smaller values. A model, which exhibits such properties, is the voltage at a point of an infinitely long RC-transmission line driven by white noise current at the the same point, or equivalently the one dimensional heat equation similarly driven. Thus the model uses partial differential equations (PDE) in time and ‘another dimension’, and it is not known of a ordinary differential equation that exhibits such characteristics. The future values of such a process depends on the values along the whole ‘other dimension’ consisting of an uncountable number of values. Although sometimes possible, PDEs often does not have good small-dimensional state-space models. At least not ones that that have good enough observability properties and lend themselves for estimation using a Kalman filter. Thus, bias instability is typically not accounted for in a Kalman filter, at the moment.

The bias instability value is said to represent the minimal residual bias after estimation (in terms of estimate standard deviation). A way to realize this (perhaps a bit informally) is to think about that the memory of such a process is uncountable. Moreover, it actually depends on the previous white noise function values as they will propagate into the ‘other dimension’. It is therefore next to impossible to get a very good estimate of this process, even if we where to know the inherent parameters. When the bias is estimated dynamically using GNSS, the residual bias is typically five to ten times larger than the bias instability. ■

10.8.3 Combining processes and the Allan deviation

A error signal typically consists of several processes. If one assumes that these are independent, then it can be shown that their Allan variance is additive. At least white noise and a bias process will need to be accommodated for real data. In addition, one might need to consider quantization noise ($\propto \tau^{-2}$), bias instability ($\propto 1$), and rate ramp ($\propto \tau^2$), dominating the Allan deviation for small,

IEEE Std 952-2020
IEEE Standard for Specifying and Testing Single-Axis Interferometric Fiber Optic Gyros

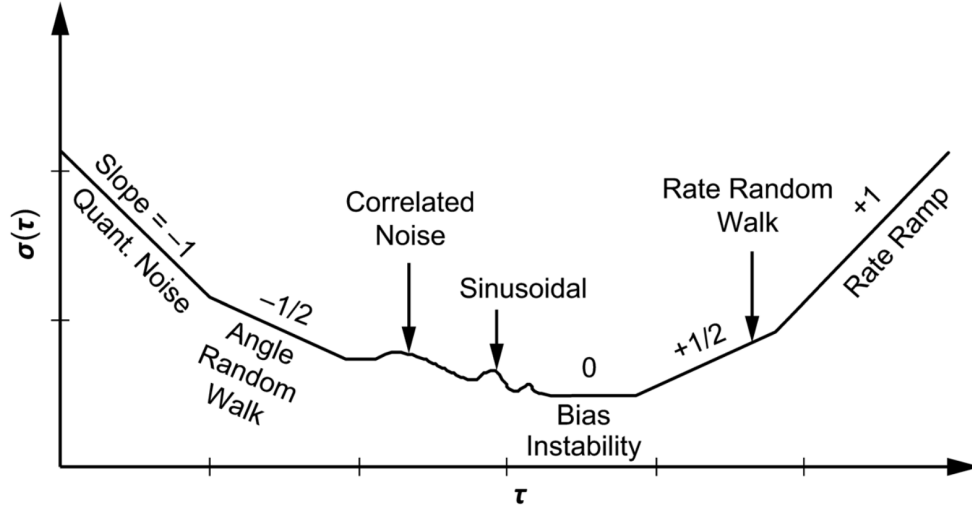


Figure 10.3: Allan deviation log-log plot example, annotated with proposed present processes. Courtesy of the IEEE standard stated above the figure.

middle and large τ , respectively. The problem with the even powered terms in the Allan variance is that they are non-stationary and without good and simple state space models, which renders them hard to estimate using, say, an extended Kalman filter.

Square root and log properties

Say you want to plot $\log_b(\sqrt{x+y}) = 0.5 \log_b(x+y)$ and $x \gg y$. Taking the Taylor series at x we get

$$\log_b(\sqrt{x+y}) \approx \frac{1}{2 \log(b)} \left(\log(x) + \frac{y}{x} \right) + o\left(\frac{y}{x}\right)^2 \approx \frac{\log(x)}{2 \log(b)}. \quad (10.18)$$

So, when plotting the Allan deviation, one might suspect that different regions of the plot are dominated by different signals. From the processes discussed above, the Allan deviation can thus be approximated as piecewise affine (straight lines) in its log-log plot.

Determining processes from the Allan deviation plot

Finding which processes are present and their parameters, is therefore about eye-balling the plot and drawing straight lines according to the processes defined above, and reading of their values.

- Extended downward slope of -0.5 means white noise or tail of a Gauss-Markov process, and σ_a or $\sigma_a \sqrt{T}$, respectively, can be read of at $\tau = 1$.
- Flat (ish) region, can mean a bias instability, where the approximate value is read of at the minimum.
- Upward slope of 0.5 means Wiener or beginning of a Gauss-Markov process, and σ_a can be read of at $\tau = 3$.
- A bump, as a shaved off 0.5 slope pyramid, can be the center of a Gauss-Markov process, and the peak point (τ_p, p) can be used to find $T = \frac{\tau_c}{1.89}$ and $\sigma_a = \frac{p}{0.437 \sqrt{T}}$.

One might, of course, consider other processes as well, but we will not investigate that here, due to the limited presence in the data and limited possibilities to easily estimate the processes ‘online’. A somewhat elaborate example of a log-log Allan deviation plot is given in figure 10.3. There quantization noise, sinusoidal noise, and rate ramp noise is considered in addition to the ones

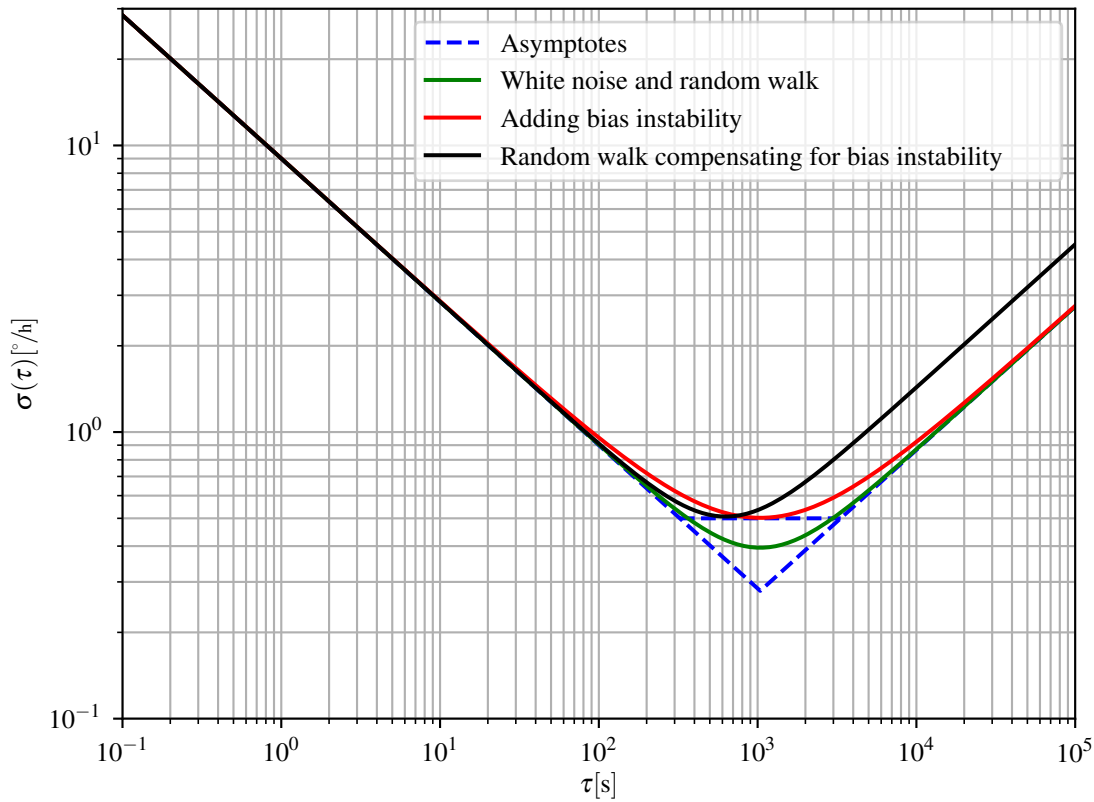


Figure 10.4: The allan deviation recreated from fitting lines to the figure in the datasheet. Asymptotes and two possible approximations are also shown.

described above. It is also important to note that the rate random walk would be indistinguishable from a Gauss-Markov process with extremely large time constant.

The modeling could also go somewhat the other way around. One can presuppose a model with parameters, and then see how a simulation or its piecewise affine approximation fits the real curve.

■ **Example 10.7** We are going to look at the allan deviation for the Sensoror STIM300 IMU gyro, and find parameters that can be used in a state filter. We are going to ignore many elements, such as scale factor error, integration errors, and temperature bias effects etc. The values for angle random walk and bias instability is taken from “Table 6-3: Functional specifications, gyros” from of the datasheet³. The value for a random walk process is approximated to extend the plot “Figure 6-5: Typical Allan-Variance of gyro” from the same datasheet. The values are⁴

- Angle random walk: $0.15^\circ/\text{h}^{0.5}$.
- Bias instability: $0.5^\circ/\text{h}$.
- Rate random walk: $0.9^\circ/\text{h}^{1.5}$

These asymptotes are shown in Figure 10.4. However, the lowest region defining the bias instability is quite close to both the white noise and random walk region, so the bias instability used in the combined plot has value $0.31^\circ/\text{h}$ instead.

A plot with the white noise and random walk, but without any bias instability, is also shown in Figure 10.4. This clearly goes too low, and leaves un-modeled noise levels. A filter would have to attribute this extra noise to something, but it is too slowly varying for white noise and too fast for

³<https://sensoror.azurewebsites.net/media/1130/ts1524-r15-datasheet-stim300.pdf>

⁴Yes, one has to take the square root of the time unit. This is, informally, due to the Wiener process having variance proportional to time, and thereby standard deviation proportional to the square root of time.

the random walk to capture it properly. This may or may not be a problem.

A remedy to capture the bias instability is to increase the driving noise of the random walk. This is done in the last plot in the figure where the noise level is $1.48^\circ/h^{1.5}$. This also increases the noise levels at long averaging times unnecessary, and too much of the fluctuations will be attributed to this process, compared to its true contribution. But, this might be a better option than not capturing it, especially considering that we still have errors that is not accounted for yet. This choice will depend on what one seeks and in relation to the errors in the approximations done in the integration of the process (which perhaps could be modeled as a random process in and of itself).

One should note, that the random walk should perhaps instead be modeled as Gauss-Markov as all proper bias processes will have finite variances. Then the Allan variance of the process in relation to the plots show that the time constant should at least be chosen larger than, say, 2×10^4 s.

The last thing to note is that the values are of rather inconvenient units. One can get the right units by scaling the y-axis in the plot by $\frac{\pi}{180 \times 3600}$ and then reading of the values again, or by inserting $^\circ = \frac{\pi}{180}$ and $h = 3600$ s into the units of values found. For instance, the angle random walk becomes $0.15^\circ/h^{0.5} = 0.15 \times \frac{\pi}{180 \times \sqrt{3600}} \text{rad}/s^{0.5} = 4.36 \times 10^{-5} \text{rad}/s^{0.5}$ when inserting for the units. ■

10.9 IMU as control input consideration

The ESKF in this book uses IMU measurements as control inputs instead of ‘normal’ measurement updates. This simplifies things a lot, since there is no need to model the acceleration process or the angular velocity process, thereby removing the need for dynamic modeling and only kinematic equations to estimate. However, the IMU measurements are not continuous, so the zero order hold approximation is taken. But how valid is this approximation? Indeed, if the conditions are wildly changing, such as for large and fluctuating jerk (time derivative of acceleration) or angular acceleration, this approximation will not be good. If the IMU measurements in addition are instantaneous, one could argue that they would be meaningless.

Therefore, we are in some sense assuming small jerk and angular acceleration compared to the sampling interval and noise magnitude. In many applications this is a valid assumption/approximation, while in some others it is not. The second thing that make this work is the fact that the measurements are often not instantaneous, but rather some form of average through signal low pass filtering in the measurement device. Low pass filtering is necessary to avoid aliasing. To remove most of the signal above the nyquist frequency, the averaging effect must be larger than the sampling frequency. This is for instance the case for the IMU STIM300 by Sensoror, where there is a 256kHz sampling internally which is digitally filtered through cascaded integrator comb like filters (effectively a time windowed integral) and decimated down to 2kHz. The acceleration/angular rate measurement is therefore for instance better thought of as the average of the true body acceleration/angular rate, IMU-noise, and -bias. Namely

$$a_m[k] = \frac{1}{t_k - t_{k-1}} \int_{t_{k-1}}^{t_k} R^T(q_t(\tau)) a_t(\tau) + n_a(\tau) + b_a(\tau) d\tau, \text{ and} \quad (10.19)$$

$$\omega_m[k] = \frac{1}{t_k - t_{k-1}} \int_{t_{k-1}}^{t_k} \omega_t(\tau) + n_\omega(\tau) + b_\omega(\tau) d\tau \quad (10.20)$$

for acceleration and angular rate, respectively.

What we are interested in is of course

$$\rho_t(t_k) = \int_{t_{k-1}}^{t_k} v_t(\tau) d\tau, \quad (10.21)$$

$$v_t(t_k) = \int_{t_{k-1}}^{t_k} a_t(\tau) d\tau + v_t(t_{k-1}) = \int_{t_{k-1}}^{t_k} R(q_t(\tau)) a_t^b(\tau) d\tau + v_t(t_{k-1}), \text{ and} \quad (10.22)$$

$$q_t(t_k) = q_t(t_{k-1}) \Delta q(t_k, t_{k-1}), \quad \frac{d}{dt} \Delta q(t, \tau) = 0.5 \Delta q(t, \tau) \omega_t(t), \quad \Delta q(\tau, \tau) = 1, \quad (10.23)$$

where $a_t^b(t)$ is the true acceleration in body coordinates.

We do not have the true values, but we have some noisy, biased and averaged measurement of a_t^b and ω_t . For estimation purposes, we settle with finding the expected values and the joint mean squared error in terms of the covariance, using of these measurements.

But what is the expected value of the rotation rate and acceleration given their average measurements? One approach that does not need any modelling, which is also often taken, is to assume that the values were constant over the integration period. This might make sense for the acceleration, but we know that the rotation rate is differentiable and thereby continuous, so this assumption is at best only mildly erroneous. If one models the angular acceleration as a white noise process, then a KF estimate for the rotation rate is after measurement in fact a quadratic in time, and the covariance a quartic. Of course, for short time steps and small angular acceleration, one can ignore this.

One takeaway from all this is that there will be integration errors Both in the mean and in the covariance. The question is only how much. When tuning the filter one will need to think about where a Kalman filter will attribute this error. One can try to capture it with both the bias process and the measurement noise, or perhaps introduce another random process altogether.

10.10 GNSS

For raw GNSS it is mainly the atmosphere variations along with the satellite orbit and clock errors that causes the errors in the pseudorange (approximate time of flight times the speed of light). The number of satellites visible along with their orbital geometry will after that determine the geometry and size of the estimated position and time error. The position and time is usually found through a (weighted) least squares procedure on the pseudoranges, and one can at the same time estimate a covariance matrix that incorporates the geometry etc.

Table 10.1 provides a list of the various errors impacting individual pseudorange measurements along with their typical values. The total error listed is the result of accumulating those individual errors in a sum-squared sense and represents the typical errors of a standalone GNSS receiver. Most receivers track SBAS satellites which provide substantial corrections to each of these terms, bringing the error down to the more commonly seen 2 m specification for consumer GNSS receivers.

Source	m RMS
Orbital	2.5
Satellite Clock	2
Receiver Noise	0.3
Ionospheric	5
Tropospheric	0.5
Multipath	1
Total	11.3

Table 10.1: Error sources in GNSS

If the receiver operates on multiple GNSS systems and multiple frequencies, more of these errors can be removed. Even more advanced differential GNSS corrections can eliminate some of these errors entirely.